Lab on a Chip

RSCPublishing

REVIEW

Lab on a chip for continuous-flow magnetic cell separation

Cite this: DOI: 10.1039/x0xx00000x

Majid Hejazian[a], Weihua Li[b], Nam-Trung Nguyen[a*]

Received 00th January 2012,
Accepted 00th January 2012

DOI: 10.1039/x0xx00000x

www.rsc.org/

Separation of cells is a key application area of lab-on-a-chip (LOC) devices. Among the various methods, magnetic separation of cells utilizing microfluidic devices offers the merits of biocompatibility, efficiency, and simplicity. This review discusses the fundamental physics involved in using magnetic force to separate particles, identifies the optimisation parameters and corresponding methods for increasing the magnetic force. The paper then elaborates the design considerations of LOC devices for continuous-flow magnetic cell separation. Examples from recently published literature illustrate these state-of-the-art techniques.

Introduction

The separation and concentration of rare cells for sample preparation is a primary step in many biological studies such as disease diagnosis.[1] Microfluidic lab-on-a-chip (LOC) devices have proven to be a promising platform for this application, owing to a number of merits such as small size, low cost, low sample and reagent consumption, portability, as well as fast analysis time.[2,3] The previous decade has witnessed an increasing trend of using LOC devices for preparing samples, isolating and analysing cells. Cells are separated based on their unique hydrodynamic, dielectrophoretic, immunochemical and magnetophoretic signatures, or a combination of these signatures.[4] Due to its non-contact nature, magnetic separation can maintain cell viability and suit well with biological investigations. On the other hand, the continuous-flow separation has a high throughput with no limits on its capacity. Other advantages include the possibility of continuous monitoring and adjusting the separation parameters, the lateral separation of sample components, and the high potential for system integration[5].

A number of reviews exist in the literature that partially includes the continuous-flow magnetic separation of cells. Radisic *et al.*[6] reviewed general cell separation concepts using micro- and nanoscale technologies. This paper briefly discussed magnetic separation with a number of examples related to cell separation. The review by Pamme[5] focused on continuous-flow magnetic separation in microfluidic devices by describing methods such as continuous-flow separation of magnetically susceptible materials, and magnetically labelled cells. Tsutsui and Ho[2] discussed cell separation methods according to various non-inertial forces, with one of the subcategories covering the continuous-flow separation of magnetically tagged cells. Liu *et al.*[7] described the physics of magnetic cell sorting and mentioned the use of LOC platforms. Bhagat *et al.*[1] reviewed several techniques and applications of microfluidic cell separation, where the concepts were categorized into passive and active techniques, and then further divided into the types of force used for separation. Magnetic cell sorting was briefly discussed through some examples. Lenshof and Laurell[8] summarised different continuous-flow separation techniques for cells and particles in microfluidic devices, including a review of the magnetic method. Gossett *et al.*[9] limited their review to label-free cell separation in microfluidic systems, where magnetic sorting as well as other several techniques was discussed. Gijs *et al.*[10] gave a comprehensive overview of the manipulation of magnetic beads in microfluidic systems and their applications in biological and chemical analysis. Zborowski and Chalmers[11] described the separation and analysis of rare cells by magnetic sorting by focusing on separation of circulating tumor cells (CTC). Another recent paper by Pamme[12] reviewed the application of magnetic particles for bioanalysis and bioprocessing within a LOC platform, recent developments in the manipulation of magnetic particles. Both magnetically functionalised droplets and magnetically labelled cells were discussed. Hyun and Jung[13] critically reviewed the microfluidic enrichments of circulating tumor cells. Several techniques for CTC isolation including magnetic separation were mentioned and categorized in this review. Chen *et al.*[4] discussed the isolation, enrichment and analysis of rare cells from an engineering perspective. Different methods based on the force used for separation, including isolation based on magnetophoretic signature, were introduced and illustrated by examples from recent published works.

The above reviews indicate that despite the significance and broad impact of microfluidic continuous-flow cell separation

based on magnetic force, none of them focused on or addressed the unique features of different magnetic separation techniques. To fill this gap, our present paper will give a concise review that focuses only on continuous-flow magnetic cell separation using microfluidic devices. The fundamental physics behind magnetic separation is first discussed, followed by a analysis on techniques that could enhance the efficiency and throughput of magnetic microfluidic cell separation. Finally, a variety of applications for these techniques will demonstrate the uniqueness and usefulness of continuous-flow magnetic separation.

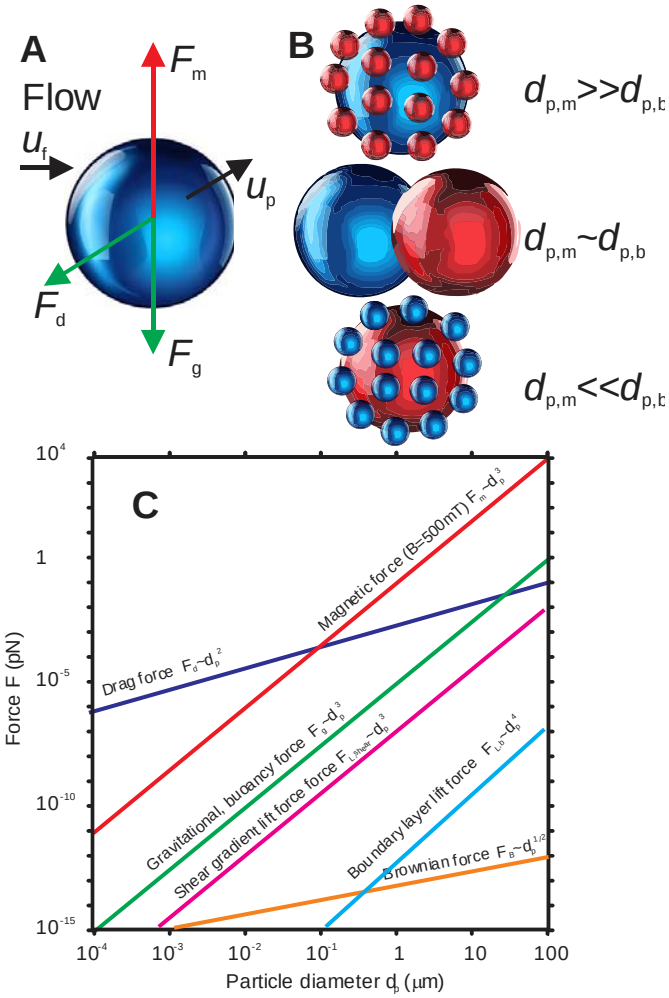

Fig. 1 Dominant forces on a particle in a flow field: (A) representative illustration of force and velocity components (the direction of $\mathbf{F}_m$ and $\mathbf{F}_g$ are arbitrary); (B) Relative sizes between magnetic particles (blue) and diamagnetic (biological) particles (red); (C) Order of magnitudes of different forces as function of characteristic particle diameters (at typical velocity of 1 mm/s and channel width and depth of 100 μm).

Physics of magnetic separation

Microfluidic magnetic separation is a subfield of micro magnetofluidics, a research field that involves the interaction between magnetism and fluid flow in microscale.[14] This section focuses on key forces that may affect particle trajectory while passing through the microfluidic device. We first need to understand the force balance acting on the particles to identify the optimisation parameters of the separation devices to increase the yield and throughput of the separation process. The order magnitude of each force is first estimated to identify the dominant forces and their related design parameters for effective separation. The trajectory of a magnetic particle in a laminar flow through a microchannel is determined by the balance of many forces, Fig. 1A. According to Newton's second law, the force balance on a moving particle is[15]:

$$m_p \frac{d\mathbf{u}_p}{dt} = \mathbf{F}_m + \mathbf{F}_g + \mathbf{F}_d + \mathbf{F}_B + \mathbf{F}_L \quad (1)$$

where m_p is the mass of particles, $\mathbf{u}_p$ is the particle velocity, $\mathbf{F}_m$, $\mathbf{F}_d$, $\mathbf{F}_g$, $\mathbf{F}_B$, $\mathbf{F}_L$ are magnetic force, drag force, gravity force, Brownian force, and lift force, respectively.

Magnetic force

The force acting on a magnetic particle within a magnetic field is[14]:

$$\mathbf{F}_m = \frac{V_p \Delta\chi}{\mu_0}(\mathbf{B}.\nabla)\mathbf{B} \quad (2)$$

where $\mathbf{F}_m$ is the magnetic force (N), V_p is the volume of the particle (m^3), $\Delta\chi = \chi_p - \chi_f$ is the difference between magnetic susceptibilities of the particles χ_p and the base fluid χ_f (dimensionless), $\mathbf{B}$ is the magnetic induction, and $\mu_0 = 4\pi \times 10^{-7}$ (TmA^{-1}) is the permeability of vacuum. The above equation indicates that a gradient in magnetic field and a susceptibility difference is required to induce a magnetic force on a particle. A torque can be generated by a uniform magnetic field, but no motion can be achieved.[14,16] Equation (2) assumes a uniform magnetisation of the bead. Considering non-uniform magnetisation, Shevkoplyas et al.[17] proposed a more general expression for the magnetic force:

$$\mathbf{F} = \rho V \nabla(\mathbf{M_0}.\mathbf{B}) + \frac{V\chi_p}{\mu_0}(\mathbf{B}.\nabla)\mathbf{B} \quad (3)$$

where ρ is the density of the bead (kg m^{-3}), $\mathbf{M}_0$ is the initial magnetization of the bead (A m^2 kg^{-1}). When the magnetization is completely saturated, the magnetic moment of the particle is not varying in space ($\nabla.m = 0$). In the case of strong spatial field variations or a Janus particle, which has different properties in each half,[18] the magnetic moment of the particles is not constant when moving in space ($\nabla.m \neq 0$), equation (3) should be considered.[19] Macroscopic permanent magnets and electromagnets can produce magnetic fields sufficiently strong (>0.5 T) to saturate the magnetization of superparamagnetic beads. Equation (2) is suitable for relatively high magnetic field strengths with the order of magnitude of saturation field strength of the magnetic bead.[17] Furthermore, equation (2) can be applied for paramagnetic, and superparamagnetic particles, where soft magnetism approximation was considered for the particles, considering the fact that these particles have no magnetic memory.[20,21] In an external magnetic field, the nanoparticles in a ferrofluid have a ferromagnetic behaviour at room temperature. Their average magnetization is zero in the absence of an external magnetic field. There is a critical diameter for nanoparticles below which the material is superparamagnetic and equation (2) is applicable.[22,16]

The gravitational force

Considering buoyancy, the gravitational force can be expressed as:

$$\mathbf{F}_g = -V_p(\rho_{P-}\rho_f)g \quad (4)$$

where $\mathbf{F}_g$ is the gravitational force, V_p, ρ_P, ρ_f and g are the volume of the particle, the density of the particle and fluid, and acceleration due to gravity, respectively.

Drag force

For a particle suspended in a fluid flow under a condition of low Reynolds numbers, the drag force is estimated from the Stokes' law and relative velocity:[23]

$$\mathbf{F}_f = 3\pi\eta d_c(\mathbf{u}_f - \mathbf{u}_p) \quad (5)$$

where η is the dynamic viscosity of the fluid, $\mathbf{u}_f$, $\mathbf{u}_p$ are the velocities of fluid and the particles, respectively. The apparent diameter of the composite particle d_c can be estimated based on the different scenarios of relative size ratio between the magnetic particles and the biological particles attached to them through affinity, Fig. 1B. In the case magnetophoreis, the motion of the particle under the magnetic force, the drag force consists of two components. One is caused by the fluid flow and opposing the flow direction. The other one is opposing the magnetic force. The net drag force opposes the resulting particle motion, Fig. 1A.

Lift force

Spherical particles experience a hydrodynamic lift force, which results in a velocity component that is perpendicular to primary streamlines. There are two types of lift forces on particles depending the position of the particle. The first one is the shear gradient induced lift force: [24]

$$\mathbf{F}_{L,s} = \frac{\pi}{8}\rho_f \boldsymbol{\omega}\mathbf{u}\, d_p^3 \quad (6)$$

The second one is the boundary layer lift force:

$$\mathbf{F}_{L,b} = 9.22\left(\frac{9}{4}\frac{U^2}{h^2}\right)\rho_f d_p^4, \quad (7)$$

where $\mathbf{F}_{L,s}$ and $\mathbf{F}_{L,b}$ are the respective shear gradient induced and boundary layer lift forces, d_p is the diameter of the particle, ρ_f is the density of the fluid, $\boldsymbol{\omega}$ *i*s the vorticity of the flow, $\mathrm{Re}_p = \frac{U\, d_p}{\nu}$ is the Reynolds number of the particle, ν is the kinematic viscosity of the fluid, U is the average velocity of the particle, and h is the channel height. For a uniform laminar flow field, the vorticity can be estimated as $\boldsymbol{\omega} = \frac{\partial u}{\partial y} = \frac{U}{h}$. The inertial force is proportional to the flow velocity and the particle size relative to the channel length. At high Reynolds numbers $\mathrm{Re}_p >> 1$, the inertial lift force becomes dominant and can be used for lateral separation of particles. At low Reynolds numbers $\mathrm{Re}_p << 1$, the viscous drag force is more significant. A relatively high velocity and large particle size are required for lift force to have a magnitude comparable with magnetic force. Thus, a separation application cannot benefit from both magnetic and inertial lift forces at the same time due the fact that magnetic separation and inertial separation are working in different ranges of velocity.[25]

Brownian force

Random collisions of molecules of the fluid with the suspended particles cause a random movement called Brownian motion. The Brownian force can be estimated as[26]:

$$\mathbf{F}_B = \zeta\sqrt{\frac{6\pi k_B \eta T\, d_p}{\Delta t}} \quad (8)$$

where k_B is the Boltzmann constant, η is fluid viscosity, T is the absolute temperature, r_p is the radius of the particle, Δt is the magnitude of the characteristic time step. The parameter ζ is a Gaussian random number with zero mean and unit variance. Brownian motion can affect the movement of particles if the radius of particles is less than the threshold diameter estimated based on the following relationship[27]:

$$|\mathbf{F}| d_p \le k_B T \quad (9)$$

where $|\mathbf{F}|$ is the magnitude of the total force acting on the particle. For particles with diameter smaller than this critical radius, trajectories cannot be evaluated by Newton's equation (1). [23]

Other forces

In addition to the forces discussed above, other forces acting on a particle in a laminar flow also exist, such as particle-particle interaction forces, Van der Waals attraction force, thermophoretic force, lift force, and magnetic and electrostatic interaction forces between particles[4]. Depending on the type of separation phenomena, these forces can be added to equation (1), and would result in a complex model, which can only be solved by numerical simulation.

Significant forces and optimisation parameters for cell separation

Many of the mentioned forces could be ignored for cell separation applications, depending on size of the particles and the magnitude of the magnetic field strength. Particle-particle and particle-fluid interactions can be ignored for particle suspensions with small particles volume concentration ($c << 1$). [23] Figure 1C illustrates schematically the order of magnitude of forces acting on a magnetic particle, based on typical conditions used in most of magnetic separation problems. Figure 1C indicates that in a relatively weak magnetic field typically generated by integrated electromagnet such as microcoil and line conductor, drag force is dominant, while gravitational and magnetic forces have comparable order of magnitude. But in a relatively high magnetic field typically generated by permanent magnets, drag force and magnetic force are the most dominant forces, and other forces could be ignored[10].

Most of the works reported in the literature only consider the two most significant forces: the drag force and the magnetic force. Considering a single spherical magnetic particle with a radius r_p in a quiescent fluid, balancing the magnetic and drag force results in the magnetophoretic velocity:[20]

$$\boldsymbol{u}_p = \frac{d_p^2(\chi_p - \chi_f)(\mathbf{B}\cdot\nabla)\mathbf{B}}{18\mu_o\eta} \quad (10)$$

This equation reveals the key parameters for designing a microfluidic device to separate cells by a relatively strong magnetic force, namely the size, the magnetic susceptibility difference, the magnetic field and field gradient and the viscosity of the surrounding fluid.

Methods to improve magnetic separation

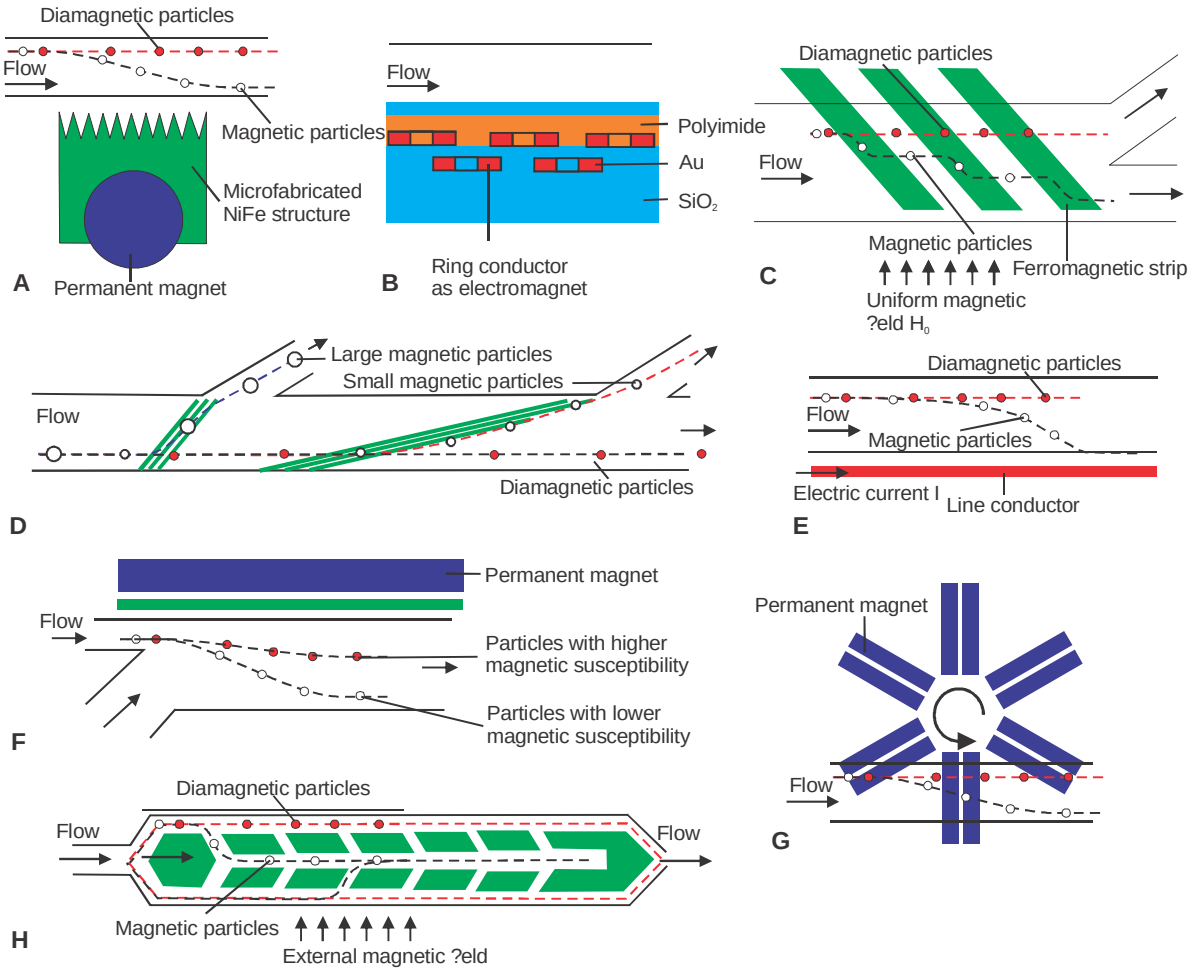

Fig. 2 Techniques for increasing magnetic field gradient: (A) Micro-comb with sharp tips to generate a non-uniform magnetic field; (B) Ring conductors to create four-phase magnetic field; (C) Angled ferromagnetic wire array used for lateral displacement; (D) Microfabricated ferromagnetic strip arrays for multitarget cell sorting; (E) Line conductor etched in copper as electromagnet; (F) A permanent magnet placed next to the Ni microstructure for magnetic gradient concentration; (G) A Spinning array of permanent magnets used in magnetic trap device; (H) A six-stage cascade paramagnetic mode magnetophoretic separation (PMMS) system for separating suspended cells in blood. Images reproduced from Ref. 28, 29, 31-33, 35, 37.

The main objective of continuous-flow separation is to attract or repel particles or cells from their regular trajectory in a fluid flow, and to guide them to a specific outlet for collection. The main challenge in designing a microfluidic device for this purpose is achieving both high efficiency and throughput. Various techniques have been applied to improve the magnitude of magnetic force relative to other forces as highlighted in the previous section. These techniques are classified and reviewed as follows.

Techniques to increase the magnetic field gradient

Equation (2) shows that the magnetic gradient ∇B is one of the key parameters for creating a larger magnetic force. Various methods for increasing the gradient have been reported in the literature. Xia *et al.*[28] used micro-comb and micro-needle structures to generate a non-uniform magnetic field, Fig. 2A. Red blood cells and E-coli cells labelled with magnetic nanoparticles were separated with high efficiency and throughput. The results showed that the micro-needle geometry concentrates the magnetic field to a single position along the channel, while the micro-comb geometry can create a gradient over a longer channel and thus provide the particles with a longer residence time in the field gradient.

High field gradient can also be achieved with small integrated electromagnets. Liu *et al.*[29] suggested using current-carrying conductors to create a higher gradient to separate particles with two different sizes, Fig. 2B. Their experimental and simulation results revealed that the combined effect of magnetic fields provided by conductors and an additional uniform external field led to higher deflections of the particle trajectories. Jung and Han [30] utilized a ferromagnetic wire array to create a high-gradient magnetic field for improving separation efficiency (up to 93.9 % for RBCs, and 89.2% for WBCs), Fig. 2C. They demonstrated a lateral-driven method for continuous magnetophoretic separation of RBCs and WBCs cells from peripheral whole blood, using their intrinsic

magnetic properties. A reasonable efficiency was achieved with the flow rate of 20 l/h and an external magnetic flux of 0.3 T. Micromachined ferromagnetic strips (MFS) were used by Adams et al.[31] to continuously and simultaneously sort two types of labelled cells (three different types of E. coli MC1061 cell labelled target buffer) into two outlets, Fig. 2D. The high magnetic field gradient created by the MFS arrays in the microchannel made it possible to control and balance the drag force and the magnetophoretic force and to guide the target cells to two outlets, with purity higher than 90% for multiple bacterial cell types, and a throughput of 10^9 cells per hour.

Because of the relatively large current needed for the electromagnet, a thick conductor is preferable for the electromagnet. Derec *et al.*[32] introduced a copper-etched microchip, where the electric current passed through a line conductor parallel to the microchannel and generated a tuneable magnetic field inside the channel, Fig. 2E. Numerical and experimental data showed that the chip was capable of performing a satisfactory extraction of tumour cells labelled with magnetic nanoparticles. The main disadvantages of this device were the heat generated by the copper conductor when exposed to an electrical current, and being unable to reduce the size of the channel any further.

The magnetic field can be concentrated using ferromagnetic structured placed next to the mirochannel. Lee *et al.*[33] devised a high-speed RNA microextractor by utilizing a lateral ferromagnetic wire array for isolating RNA from human blood lysate using magnetic oligo-dT. A ferromagnetic wire array was placed at an angle proportionate to the direction of flow under an applied external magnetic field. The ferromagnetic wire array was able to produce a high-gradient magnetic field that directed the tagged particles to the collecting outlet. This device could separate more than 80% of the magnetic beads with a flow rate up to 20 ml h^{-1}, in only one minute. Shen *et al.*[34] placed a ferromagnetic wire beneath a microchannel to generate a magnetic gradient from an external uniform magnetic field, Fig. 2F. The device successfully separated red and white blood cells whole blood based on their native magnetic properties.

Most reported works used a stationary permanent magnet to induce the magnetic field into the microfluidic device. A time-dependent magnetic field is able to induce a time-varying particle velocity, and thus an additional inertial force for faster trapping and separation. Verbarg *et al.*[35] utilised a spinning magnetic trap to make a "MagTrap" device, Fig. 2G. A rotating magnet wheel enables a magnetic gradient to trap, mix and release the targeted cells. The device was capable of performing automated target capture, efficient mixing with reagents, and separation in a single microfluidic channel.

The external magnetic field can be further optimized by arranging the permanent magnet so the position of maximum field gradient in the microchannel can be adjusted. Wilbanks et al.[36] conducted an experimental and theoretical study to investigate the effects of magnet arrangement on trapping of diamagnetic particles in ferrofluid flow through a straight rectangular microchannel. Positioning the magnets around a microchannel asymmetrically increases the rate for particle trapping.

If the deflection of particles through magnetophoresis is not large enough, cascading multiple separation units could bring better separation results. Jung *et al.*[37] developed a six-stage cascade paramagnetic mode magnetophoretic separation (PMMS) system for the separation of red blood cells from human whole blood, using their native magnetic properties, Fig. 2H. The cascade ferromagnetic structures created a high magnetic gradient allowing a high throughput up to 50.4 μL/hr and an efficiency of 86.2 %. Processing 5.0 μL blood sample only needs 6.0 min. Lee *et al.*[38] used magnetic nanoparticles (MNPs) modified with bis-Zn-DPA to remove both Gram-negative bacteria and endotoxins from blood. By using multiple microfluidic devices in series, the MNPs bound to Escherichia coli were successfully removed from bovine whole blood, with almost 100% clearance. Khashan *et al.*[39] proposed a microfluidic design for the separation of magnetically labelled bio-particles based on numerical simulation. Integrated soft-magnetic elements intersecting the flow were considered to overcome the disadvantage of short-range magnetic force and the limitation of channel size. The proposed scheme improved the capture efficiency quite significantly compared to systems with magnetic structures embedded in the channel wall.

Many microfluidic devices are made of Polydimethylsiloxane (PDMS). Thus, mixing magnetic materials with PDMS to form microstructure with higher magnetic susceptibility would allow integrating field gradient enhancing structures into a microfluidic device made of PDMS. Gelszinnis et al.[40] reported magnetophoretic manipulation in microsystem using I-PDMS microstructures, which is made of carbonyl iron microparticles mixed in a PDMS matrix. The magnetic composite structures generated locally high magnetic field gradients when placed between two permanent magnets, and are suitable for capturing and sorting of magnetic species with different magnetic properties.

Techniques to increase the susceptibility mismatch

According to Equation (2), the susceptibility mismatch is another significant parameter that practically can lead to higher separation efficiency and/or throughput. Modifying either the susceptibility of the particle or the surrounding fluid can create the desired susceptibility mismatch. Labelling the target cells with particles of high magnetic susceptibility and modifying the susceptibility of the medium are two possible approaches to increase the susceptibility difference. In order to magnetically separate cells, which are commonly diamagnetic, a modification of their magnetic properties is required. Attaching cells to magnetic beads is an established method that has been well reported in the literature. The size of the magnetic particle and the effective size of the composite particle are important parameters for effective separation. As illustrated in Figure 1B, three cases could be considered based on the relative size ratio of the beads and the cells. (i) If the size of the magnetic bead is significantly larger than the size of cells, and a single bead is surrounded by many cells, the volume for a spherical bead ($V_p = {}^1\!/_6\,\pi d_p^3$) can be used in equation (2) to evaluate the magnetic force. (ii) If the diameters of the cell and the bead are comparable, the magnetic force exerted on the bead is calculated with equation (2), while the movement of the cell-bead complex is affected by counteracting drag force on the composite particle, and is more complicated to predict.[41] (iii) If the size of cell is significantly larger than the size of the magnetic beads, the magnetic force is small relative to the drag force and a strong magnetic field gradient or a higher

concentration of tagged magnetic particles are needed for effective separation.

Kim et al.[42] devised an immune-magnetophoresis (IMP) cell sorting chip to separate T-cells from biological suspensions using magnetic particles as tags. The cells and antibody coated magnetic particles are introduced via two separate inputs, and bind together as they move through the microchannel. The labelled cells are then attracted to a permanent magnet, and separated from the solution. Both binding and separation was executed in a simple and straight microchannel, Fig. 3. Pamme and Wilhelm[43] investigated the continuous magnetic sorting of mousemacrophages and human ovarian cancer cells (HeLa cells) that were internally labelled with magnetic nanoparticles. The cells were separated from each other depending on their size and magnetic loading. The theoretical prediction agreed with the experimental data.

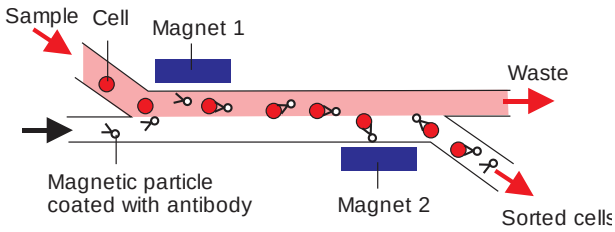

Fig. 3 Labelling cells to increase susceptibility. A micro immune-magnetophoresis cell sorter with both tagging and separation performed within the microchannel, reproduced from 42.

Shih et al.[44] examined the separation of bacteria bound to magnetic sugar-encapsulated nanoparticles. They concluded that the flow rate and the strength of the magnetic field were significant variables affecting efficiency. The most efficient sorting they could achieve was more than 90% with a selectivity of about 100%. Forbes and Forry[45] performed a numerical, analytical and experimental analysis of the lateral magnetophoretic deflection of magnetically labelled breast adenocarcinoma MCF-7 cells on a chip. Using the design tool, the necessary beads, magnet configuration (orientation), magnet type (permanent, ferromagnetic, electromagnet), flow rate, channel geometry, and buffer to achieve the desired level of magnetophoretic deflection or capture, could be identified and used for optimizing the separation process. This paper introduced a dimensionless magnetophoresis number to characterize the transition between the hydrodynamically dominated regime and the magnetically dominated one.

Tagging cells with magnetic particles required affinity binding reaction and the preparation of particles, a separation process without the need of magnetic tags would be simpler and at a lower cost to implement. Thus, modifying the susceptibility of the surrounding fluid also increases the susceptibility difference and results in a higher magnetic force. Shen et al.[34] utilised biocompatible gadolinium diethylenetriamine pentaacetic acid (Gd−DTPA) for this purpose. In their experiment, label-free U937 cells were separated from red blood cells (RBCs) with a purity higher than 90% and a throughput of 1×10^5 cells/h using a 40-mM Gd−DTPA solution.

Adding ferrofluid, a liquid with suspended magnetic nanoparticles, to the sample also increase the mismatch in magnetic susceptibility. Zeng *et al.*[46] investigated the magnetophoretic separation of diamagnetic polystyrene particles and live yeast cells in a ferrofluid solution, Fig. 4A. The predicted trajectory of cells and particles from numerical simulation agreed well with the experimental results. Furthermore, the viability test for the yeast cells after separation demonstrated the reasonable biocompatibility of the diluted ferrofluid.

The increase in susceptibility of the carrier liquid such as ferrofluid allows both positive and negative mismatch making magnetophoretic separation of both diamagnetic and magnetic particles possible. Liang et al.[47] investigated the simultaneous positive and negative magnetophoresis of magnetic and diamagnetic particles in a ferrofluid, Fig. 4B. Particle transport in both ferrofluid- and water-based separations was experimentally and analytically investigated. Using a T-microchannel, ferrofluid-based magnetic separation can offer a significantly higher particle throughput than the water-based separation due to an induced negative magnetophoresis of diamagnetic particles in the ferrofluid.

Zhu et al.[48] used water-based ferrofluids to increase the susceptibility difference to separate diamagnetic particles of different sizes. A minimum throughput of 10^5 particles/h and close to 100% separation of microparticles were achieved, Fig. 4C. Zhu et al.[49] developed an analytical model, along with experimental verifications, of transport of nonmagnetic spherical microparticles in ferrofluids in a microfluidic system that consists of a microchannel and a permanent magnet, Fig. 4D. Larger particles were further deflected perpendicular to the flow. The deflection of particles could be increased by lowering the flow rates in the microchannel.

Cheng *et al.*[50] developed a 3D analytical model to study microfluidic motions of diamagnetic particles in magnetic fluids. The model could be used to study the trajectories of the particles in the channel. The effects of flow rate, susceptibilities of particles and the base fluid, as well as different geometrical parameters of the system on the magnitude of particle deflection were investigated. Zhu *et al.*[51] suggested a new separation method that combines both positive and negative magnetophoresis based on ferrofluids for separating magnetic and diamagnetic particles, as well as particles with different magnetizations, Fig. 4E. The basic concept is to use a ferrofluid with susceptibility between those of the particles.

Liang *et al.*[52] experimentally and theoretically investigated diamagnetic particle deflection in ferrofluid flow through a rectangular microchannel. It is found that diamagnetic particles can be moved both outwards and downwards over the channel cross-section to form a focused particle stream. Particle deflection across the channel width could be increased with the decreasing flow rate, increasing ferrofluid concentration and increasing particle size. Liang and Xuan[53] suggested continuous sheath-free magnetic separation of particles in a U-shaped microchannel. Magnetophoresis focuses polystyrene particles of different sizes in a diluted ferrofluid and separates them in two branches of a U-shaped microchannel.

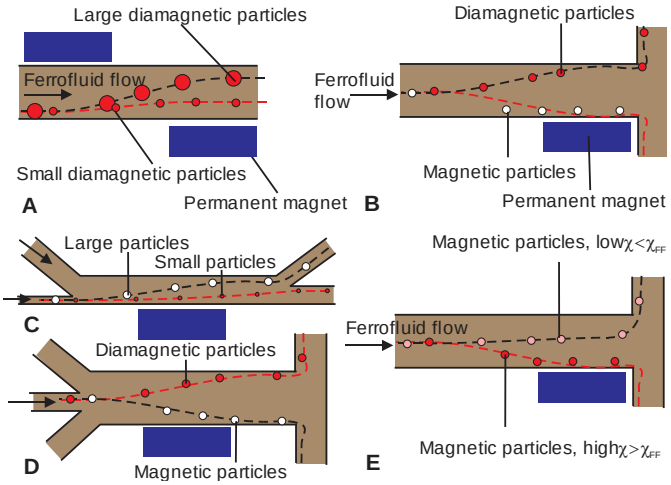

Fig. 4 Magnetophoresis with ferrofluid.

Zeng *et al.*[54] presented three-dimensional magnetic focusing of particles and cells in ferrofluid flow through a straight microchannel. Two symmetrically repulsive permanent magnets were embedded adjutant to a straight rectangular microchannel in a PDMS-based microfluidic device. Magnetic focusing of polystyrene particles in ferrofluid was observed three-dimensionally, with both top- and side-view visualizations. The effects of flow speed and particle size on the effectiveness of particle focusing were studied. Diamagnetic particle focusing in ferrofluid is enhanced with decreasing flow speed and/or increasing particle size.

Besides ferrofluid, some salt solutions can also be used as the paramagnetic carrier fluid for diamagnetic separation. Zhu *et al.*[55] developed on-chip manipulation of diamagnetic particles in paramagnetic solutions using embedded permanent magnets. Manganese (II) chloride ($MnCl_2$) solutions as carrier fluid creates enough susceptibility difference for sorting of polystyrene particles. The effects of particle position (relative to the magnet), particle size, $MnCl_2$ salt concentration, and fluid flow velocity on the horizontal magnetophoretic deflection are examined using a combined experimental and theoretical approach.

Negative magnetophoresis can be extended to particle focusing and concentrating, where diamagnetic particles suspended in a magnetic fluid are trapped at places with the lowest magnetic field gradient. Zeng et al.[56] investigated magnetic concentration of polystyrene particles and live yeast cells in ferrofluid flow through a straight rectangular microchannel using negative magnetophoresis. Two attracting permanent magnets placed on the top and bottom of the planar microfluidic device and held in position by their natural attractive force were used to create a magnetic field gradient. They could successfully separate yeast cells, without significant biological harm, from the polystyrene particles. Some of the main techniques for increasing magnetic and/or susceptibility mismatch are summarized in Table 1.

Table 1 Summary of various methods for increasing magnetic field gradient and susceptibility mismatch

Magnetic field gradient	Susceptibility mismatch	Type of cells	Ref.
Copper conductor	Magnetic tags	Tumour cells	32
Array of magnetized Elements	NA	RBCs and WBCs	16
Ni wire	Paramagnetic salt	U937 cells from RBCs	34
Ferromagnetic wire array	Magnetic tags	RNA	33
Rotating magnets	Magnetic tags	E. coli	35
Ferromagnetic strips	Magnetic tags	E. coli	31
NA	Water-based ferrofluid	Live yeast cells	40
Permanent magnets	Magnetic tags	E coli	37
Magnetized NiFe microcomb	Magnetic tags	E-coli and RBC	28

Hybrid techniques

If other non-magnetic properties of the particles are considered, other methods could be combined with separation based on the magnetophoretic property to further increase efficiency and throughput. Kim and Soh[57] utilized an integrated Dielectrophoretic–Magnetic Activated Cell Sorter (iDMACS) to take advantage of dielectrophoresis and magnetophoresis forces to sort multiple bacterial cell types in a single pass, Fig. 5A. Three different bacterial clones of E. coli MC1061 strain were used in these separation experiments. The use of two distinct force fields completely eliminated any cross-contamination of target cell types between the two outlets. The use of both force fields has the benefit of removing the cross-contamination of target cell types between the two outlets leading to a high purity separation. Up to 3000-fold enrichment of tags, and a 900-fold enrichment of bacterial cells at a throughput of 2.5×10^7 cells/h were achieved.

Seo *et al.*[58] proposed a hybrid cell sorter that exploits both hydrodynamics and magnetophoresis for sorting Jurkat cells, and red and white blood cells. The classification efficiency of Jurkat cells and white blood cells dropped with the hybrid scheme, compared to the inertial force-based separation method. Yet, an increase from 75.2 to 86.8% in efficiency was observed for the red blood cells, with the hybrid design. Siegrist *et al.*[57] exploited centrifugal and magnetophoretic forces to separate magnetic particles of different sizes, as well as magnetic and diamagnetic particles of the same size. They achieved an average separation of 75% of the larger magnetic particles. Mizuno *et al.*[60] introduced a microfluidic system that utilises both hydrodynamic and magnetophoretic forces to sort the tagged JM cells and HeLa cells, based on their size and magnetophoretic property, Fig. 5B. In the first stage, the cells were focused onto one sidewall by the hydrodynamic effect, and sorted into different outlets based on their size difference.

In the second stage, the outlets were exposed to a permeant magnet, and cells were separated through multiple outlet branches on the basis of their magnetophoretic characteristic. A high efficiency of 90% was achieved.

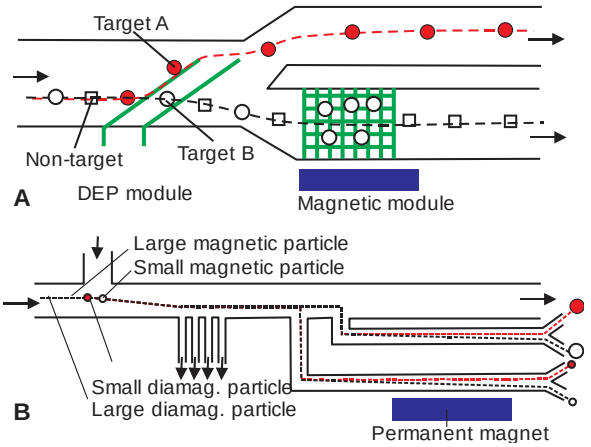

Fig. 5 Hybrid techniques: (A) Dielectrophoresis and magnetic separation;[57] (B) Hydrodynamic filtration and magnetophoresis[60].

Sajay *et al.*[61] proposed a microfluidic platform for negative enrichment of circulating tumour cells (CTC). A two-step depletion process was used. An upstream immunomagnetic depletion first separates CD45-positive WBCs. And then a microfabricated filter membrane performs chemical-free RBC depletion and target cells isolation. The micro slit membrane was designed to allow a selective passage of RBCs and platelets while retaining nucleated cells. This method was able to separate WBCs and RBCs with more than 90% WBC depletion and more than 90 % recovery of CTCs.

Applications of continuous-flow magnetic separation

Since cells in a sample are often rare and needed to be isolated for subsequent processes, an efficient separation should not jeopardize their viability. Magnetic separation techniques are biocompatible and gentle, so any damage caused by forces acting on the cells is negligible.[4] For this reason, microfluidic magnetic separation techniques for biological particles have recently become a hot research topic. As already discussed in the previous section, various methods to achieve a higher efficiency for continuous cell/particle separation are available. This section introduces the remaining works in the literature on continuous-flow cell separation using magnetic force, to highlight the potential impact of magnetic separation technique on biological studies.

Blood cells

About 45% by volume of mammalian blood consists of red blood cells (RBC, erythrocytes), white blood cells (WBC, leukocytes), and platelets (thrombocytes). The remaining 55% of the volume consists of a liquid medium called plasma.[62] Separating and enriching cells in blood could be used to detect several diseases such as cancer, HIV, and malaria etc. Knowing the properties of blood cells is therefore crucial for designing a separation device. Deoxygenated haemoglobin proteins make RBCs paramagnetic, allowing them to be separated without magnetic labels, whereas other blood cells are diamagnetic. The physical properties of blood components are presented in Table 2.[63]

Table 2 Physical properties of blood components[63].

Types	Radius (μm)	Susceptibility	Density (kgm^{-3})	Viscosity ($kg\ s^{-1}$)
WBC	5.00	$-(9.2 \text{ to } 9.9) \times 10^{-6}$	1070	NA
RBC	3.84	$\chi_{rbc,oxy} = -9.22 \times 10^{-6}$ $\chi_{rbc,deoxy} = -3.9 \times 10^{-6}$	1100	NA
Plasma	NA	$-7.7 \times 10-6$	1000	0.001

Magnetic separation of blood cells using microfluidic devices have been reported previously. For instance, Furlani[36] proposed a label-free continuous method for sorting red and white blood cells in plasma, using a microdevice and magnetic force. A mathematical model was also developed to predict the transport and separation of blood cells. In two separate works, Seo *et al.*[58, 64] presented a hybrid method to separate RBCs and WBCs, using hydrodynamics and magnetophoresis. The experimental results revealed that the separation efficiency can be tuned by the magnetophoretic force.

Han and Frazier[65] reported the use of continuous-flow magnetophoretic separation to separate RBCs and WBCs from whole blood in a microfluidic device. Analytical model, numerical simulation, and experimental data confirmed that the concept is practical. In another work[66] the same team compared the diamagnetic and paramagnetic capture modes. Both methods were able to extract WBCs from whole blood with a high concentration.

Cancer cells

The presence of circulating tumour cells (CTCs) in the blood stream is a sign of either primary tumour or metastases. Spreading of CTCs could lead to creation of tumours in other organs. CTC capture is a significant step in primary diagnosis and to discover personalized drugs[13,67,68]. To separate CTCs magnetically, it is often necessary to label them with magnetic beads. Plouffe *et al.*[69] devised a microfluidic device for separating cancer cells from suspension as well as high-purity isolation of spiked cancer cells directly from whole blood. The device was able to isolate hematopoietic stem cells and endothelial progenitor cells from whole blood. The device was reported as a viable platform for high purity, efficient, and rapid sorting of rare cells directly from whole blood samples.

Hoshino *et al.*[70] examined the magnetic separation of cancer cells labelled with magnetic nanoparticles in a microdevice, where capture rates of 90% and 86% for COLO205 and SKBR3 cells were reported, respectively. A non-labelled method has been reported by Han *et al.*[71]. Continuous paramagnetic capture mode (PMC) of magnetophoretic microseparator first separate RBC from peripheral blood usingh a 0.2 T external permanent magnet. The remaining nucleated celss are subsequently detected by electrical impedance spectroscopy. About 94.8% of breast cancer cells from a sample of spiked blood were successfully separated and detected.

Bacteria

Escherichia coli (E. coli) are a Gram-negative bacterium which causes a serious and deadly disease and is highly infectious. The four strains of E. coli that cause the disease are enteropathogenic E. coli, enteroinvasive E. coli, enterotoxigenic E. coli and enterohemorrhagic E. coli. Magnetic isolation of E-coli requires tagging them with magnetic beads.[31,72] Zhu *et al.*[73] devised a microfluidic device to separate two species of cells, including E. coli and Saccharomyces cerevisiae, as well as fluorescent polystyrene microparticles, with a throughput of 10^7 cells/h, and an efficiency close to 100%. Yassine et al.[74] developed a magnetic microfluidic chip, which enabled the trapping and isolation of E. coli by tagging them with superparamagnetic beads. Soft ferromagnetic disks were used for trapping of the tagged cells in a microchannel. The particles were subsequently separated into two side chambers.

Other cell types

Continuous magnetic separation has been used to sort and isolate a variety of rare cells. This section discusses related works reported in the literature to demonstrate the broad application of continuous-flow magnetic separation. Rodriguez-Villarreal et al. [75] reported a microfluidic device based on diamagnetic repulsion to focus label-free HaCaT cells in a continuous flow. Focusing living cells was achieved using diamagnetic repulsion forces provided by paramagnetic $MnCl_2$ solution and simple permanent magnets. Robert *et al.*[76] studied the sorting of monocytes and macrophages which internalise nanoparticles to different extents based on their endocytotic capacity. Five subpopulations of narrow iron loading distributions were successfully sorted with a purity of more than 88% and an efficacy of more than 60%.

Malaria parasite digests haemoglobin in RBC and produces an insoluble crystalline byproduct called hemozoin. Infected RBCs containing hemozoin have paramagnetic characteristics an can be separated by magnetophoresis. Nam *et al.*[77] proposed a label-free method to separate not only late-stage but also early-stage malaria infected RBCs. An efficiency of approximately 99.2%, a recovery rate of approximately 98.3% for late-stage infected RBCs, and a recovery rate of 73% for early-stage infected RBCs were achieved.

Most other cells need to be tagged with magnetic beads to be handled with an external magnetic field. A centrifugo-magnetophoretic purification separation system for sorting HIV/AIDS relevant epitope (CD4) using magnetic beads as tags from whole blood was proposed by Glynn *et al.*.[78] An efficiency of up to 92% was achieved with the system. Karle *et al.*[79] demonstrated the continuous extraction and purification of E. coli DNA bound to magnetic beads in a microfluidic platform. All the essential unit operations (DNA binding, sample washing and DNA elution) were integrated onto one single chip. The magnetic beads were separated and transported using a rotating permamnent magnet.[80] Mizuno *et al.*[81] demonstrated a microfluidic system for sorting of JM cells (human lymphocyte cell line) using anti-CD4 immunomagnetic beads. The device could achieve a throughput of approximately 100 cells/s, and high purification ratios of more than 90%. Han *et al.*[82] presented an on-chip integrated RT-PCR microchip for integration of mRNA extraction, cDNA synthesis, and gene amplification. Implementing the lateral magnetophoretic technique with magnetic oligo-dT beads allowed the mRNA from small sample quantities of lysate to be extracted within one minute.

Durdik *et al.*[83] used the finite element method to proposed and analyse an integrated microfluidic system for combined magnetic cell separation, electroporation, and magnetofection. The numerical simulation indicates that the proposed method could be used to separate two types of magnetic particles: magnetically labelled cells and magnetically labelled genetic material, e.g. plasmid DNA or siRNA. Sousa *et al.*[84] presented a microfluidic device for magnetic separation of undifferentiated mouse Embryonic Stem (ES) cells from Neural Progenitor Cultures. Their model could be used for the direct application in the purification of a human neural progenitor's population of cells from pluripotent tumorogenic cells. A purity ranging from 95% to 99.5% was achieved.

Jung *et al.*[85] designed a microfluidic device for continuous magnetic sorting of the heterogeneous cancerous cells (head and neck cells lines 212LN and 686LN-M4E), tagged with magnetic nanoparticles. From their experiment, at flow rates of 100 μL/hr and 200 μL/hr, 86.3% and 79.0% of tagged cancer cells were attracted toward the centre outlet respectively, while 95.1% and 87.2% of non-tagged cells remained in the side outlets.

Conclusion and Perspectives

This review highlights the state-of-the-art techniques and applications of continuous magnetic separation of cells in a microfluidic device. Due to distinctions in the type of cells, geometry of microchannels, and different arrangements and size of magnets, a quantitative comparison of the efficiency of these methods is not possible. Handling cells tagged to magnetic bead is an established method. The availability of a wide range of immunomagnetic beads make separation with the help of magnetic bead an easy option. With further optimization, the separation systems introduced in this paper could lead to a reasonably high efficiency, throughput and purity. We recommend a numerical study as a proper guide for an effective design before fabricating the microfluidic device and a tool to optimise and save time and costs for experiments. Identifying the significant optimisation parameters introduced in this paper will lead to a higher magnetic force, and consequently a higher efficiency and throughput of assays relying on magnetic beads.

If the cost of labelled magnetic beads is a factor to be considered, label-free magnetic separation is an attractive option. Although initial works have been reported, the migration of diamagnetic microparticles in a magnetic fluid, also called diamagnetophoresis or negative magnetophoresis, has not been fully exploited. The use of a magnetization gradient for separation of diamagnetic particles may promise a huge application potential. A magnetization gradient in the carrier fluid can be easily formed by controlling the concentration distribution of paramagnetic particles or ions in carrier such as ferrofluid or $MgCl_2$ solution. On the one hand, the combination with other diamagnetic techniques to increase the force on cells could further improve the device performance. On the other hand, magnetic methods can complement other high-throughput techniques such as inertial microfluidics for a more precise control and higher efficiency. In inertial microfluidics for instance, magnetic force can be

used to switch particles from one equilibrium position to another for better separation results. The knowledge of several magnetic separation techniques and their possible applications presented here could assist the development of new ideas for future research in this field.

Acknowledgements

The authors acknowledge the start-up grant of Griffith University to NTN and the international PhD scholarship to MH.

Notes and references

[a] Queensland Micro and Nanotechnology Centre, Griffith University, Brisbane, QLD 4111, Australia.
[b] School of Mechanical, Materials and Mechatronic Engineering, University of Wollongong, Wollongong, NSW 2522, Australia.

† Footnotes should appear here. These might include comments relevant to but not central to the matter under discussion, limited experimental and spectral data, and crystallographic data.
Electronic Supplementary Information (ESI) available: [details of any supplementary information available should be included here]. See DOI: 10.1039/b000000x/

References

1. A. A. S. Bhagat, H. Bow, H. W. Hou, S. J. Tan, J. Han and C. T. Lim, *Med Biol Eng Comput*, 2010, 48, 999–1014.
2. H. Tsutsui and C.-M. Ho, *Mech Res Commun.*, 2009, 36, 92–103.
3. V. Sahore and I. Fritsch, *American Chemical Society*, 2013, 85, 11809−11816.
4. Y. Chen, P. Li, P.-H. Huang, Y. Xie, J. D. Mai, L. Wang, N.-T. Nguyen and T. J. Huang, *Lab on a Chip*, 2014, 14, 626–645.
5. N. Pamme, *Lab on a Chip*, 2007, 7, 1644–1659.
6. M. Radisic, R. K. Iyer and S. K. Murthy, *International Journal of Nanomedicine*, 2006, 1, 3 –14.
7. C. Liu, T. Stakenborg, S. Peeters and L. Lagae, *Journal of Applied Physics*, 2009, 105, 102014.
8. A. Lenshof and T. Laurell, *Chemical Society Reviews*, 2009, 39, 1203–1217.
9. D. R. Gossett, W. M. Weaver, A. J. Mach, S. C. Hur, H. T. K. Tse, W. Lee, H. Amini and D. D. Carlo, *Anal Bioanal Chem*, 2010, 397, 3249–3267.
10. M. A. M. Gijs, F. Lacharme and U. Lehmann, *Chem. Rev.*, 2010, 110, 1518–1563.
11. M. Zborowski and J. J. Chalmers, *Analytical Chemistry*, 2011, 83, 8050–8056.
12. N. Pamme, *Current Opinion in Chemical Biology*, 2012, 16, 436–443.
13. K.-A. Hyun and H.-I. Jung, *Lab on a Chip*, 2014, 14, 45–56.
14. N.-T. Nguyen, *Microfluid Nanofluid*, 2012, 12, 1-16.
15. F. Chaumeil and M. Crapper, *Particuology*, 2013, 15, 94–106.
16 Q. A. Pankhurst, J. Connolly, S. K. Jones and J Dobson, J. Phys. D: Appl. Phys. 2003, 36, R167–R181.
17. S. S. Shevkoplyas, A. C. Siegel, R. M. Westervelt, M. G. Prentissc and G. M. Whitesides, Lab Chip, 2007, 7, 1294–1302.
18. H. Yabu, H. Ohshima, and Y. Saito, ACS Appl. Mater. Interfaces, 2014, 6, 18122–18128.
19. M. A. M. Gijs, *Microfluid Nanofluid*, 2004, 1, 22–40.
20. N. Pamme, Lab Chip, 2006, 6, 24-38.
21. T. Baier, S. Mohanty, K. S. Drese, F. Rampf, J. Kim, F. Schonfeld, Microfluid Nanofluid, 2009, 7, 205–216.
22. S. Singamaneni, V. N. Bliznyuk, C. Binekc and E. Y. Tsymbal, , J. Mater. Chem., 2011, 21, 16819.
23. E. P. Furlani, *Journal of physics, 2006, 99, 024912.*
24. J. Berthier, and P. Silberzan, Microfluidics for biotechnology, 2nd edition, 2010, ARTECH HOUSE
25. J. S. Park, S. H. Song, and H. I. Jung, Lab Chip, 2009, 9, 939–948.
26. M. M. Kim and A. L. Zydney, *Journal of Colloid and Interface Science*, 2004, 269, 425–431.
27. R. Gerber, R. M. Takayasu, and F. J. Friedlander, IEEE Trans. Magn., 1983, 19, 2115.
28. N. Xia, T. P. Hunt, B. T. Mayers, E. Alsberg, G. M. Whitesides, R. M. Westervelt and D. E. Ingber, *Biomed Microdevices*, 2006, 8, 299–308.
29. C. Liu, L. Lagae, R. Wirix-Speetjens and G. Borghs, *Journal of Applied Physics*, 2007, 101, 024913.
30. J. Jung and K.-H. Han, *Applied Physics Letters*, 2008, 93, 223902.
31. J. D. Adams, U. Kim and H. T. Soh, *PNAS*, 2008, 105, 18165–18170.
32. C. Derec, C. Wilhelm, J. Servais and J.-C. Bacri, *Microfluid Nanofluid*, 2010, 8, 123–130.
33. H. Lee, J. Jung, S.-I. Han and K.-H. Han, *Lab on a Chip*, 2010, 10, 2764–2770.
34. F. Shen, H. Hwang, Y. Ki Hahn and J.-K. Park, *Analytical Chemistry*, 2012, 84, 3075−3081.
35. J. Verbarg, K. Kamgar-Parsi, A. R. Shields, P. B. Howell Jr. and F. S. Ligler, *Lab Chip.*, 2012, 12, 1793–1799.
36. J. J. Wilbanks, G. Kiessling, J. Zeng, C. Zhang, T.-R. Tzeng and X. Xuan, *Journal of Applied Physics*, 2014, 115, 044901-044907.
37. Y. Jung, Y. Choi, K.-H. Han and A. B. Frazier, *Biomed Microdevices*, 2010, 12, 637–645.
38. J.-J. Lee, K. J. Jeong, M. Hashimoto, A. H. Kwon, A. Rwei, S. A. Shankarappa, J. H. Tsui and D. S. Kohane, *Nano Letters*, 2013, 14, 1−5.
39. S. A. Khashan, A. Alazzam and E. P. Furlani, *SCIENTIFIC REPORTS*, 2014, 4, 1-9.
40. R. Gelszinnis, M. Faivre, J. Degouttes, N. Terrier, R. Ferrigno and A.-L. Deman, *17th International Conference on Miniaturized Systems for Chemistry and Life Sciences 27-31 October 2013, Freiburg, Germany*.
41. B. Babic, R. Ghai, and K. Dimitrov, Proc. SPIE 6799, BioMEMS and Nanotechnology III, 67990U (December 27, 2007).
42. J. Kim, U. Steinfeld, H.-H. Lee and H. Seidel, *IEEE SENSORS IEEE SENSORS 2007 Conference*, 2007.
43. N. Pamme and C. Wilhelm, *Lab on a Chip*, 2006, 6, 974–980.
44. P. H. Shih, J.-Y. Shiu, P.-C. Lin, C.-C. Lin, T. Veres and P. Chen, *JOURNAL OF APPLIED PHYSICS*, 2008, 103, 07A316.
45. T. P. Forbes and S. P. Forry, *Lab Chip*, 2012, 12, 1471–1479.
46. J. Zeng, Y. Deng, P. Vedantam , T.-R. Tzeng and X. Xuan, *Journal ofMagnetismandMagneticMaterials*, 2013, 346, 118–123.
47. L. Liang, C. Zhang and X. Xuan, *Appl. Phys. Lett.*, 2013, 102, 234101-234104.
48. T. Zhu, F. Marrero and L. Mao, *Microfluid Nanofluid*, 2010, 9, 1003–1009.
49. T. Zhu, D. J. Lichlyter, M. A. Haidekker and L. Mao, *Microfluid Nanofluid*, 2011, 10, 1233–1245.
50. R. Cheng , T. Zhu and L. Mao, *Microfluid Nanofluid*, 2014, 16, 1143–1154.
51. T. Zhu, R. Cheng, Y. Liu , J. He and L. Mao, *Microfluid Nanofluid*, 2014, DOI: 10.1007/s10404-014-1396-9.
52. L. Liang, J. Zhu and X. Xuan, *BIOMICROFLUIDICS*, 2011, 5.
53. L. Liang and X. Xuan, *Biomicrofluidics*, 2012, 6.
54. J. Zeng, C. Chen, P. Vedantam, V. Brown, T.-R. J. Tzeng and X. Xuan, *J. Micromech. Microeng.*, 2012, 22.
55. J. Zhu, L. Liang, X. Xuan, *Microfluid Nanofluid*, 2012, 12, 65–73.
56. J. Zeng, C. Chen, P. Vedantam, T.-R. Tzeng and X. Xuan, *Microfluid Nanofluid*, 2013, 15, 49–55.
57. U. Kim and H. T. Soh, *Lab on a Chip*, 2009, 9, 2313–2318.
58. H.-K. Seo, Y.-H. Kim, H.-O. Kim and Y.-J. Kim, *J. Micromech. Microeng.*, 2010, 20.
59. J. Siegrist, L. Zavattoni, R. Burger and J. Ducrée, *Transducers'1111, Beijing, China, June 5-9*, 2011.
60. M. Mizuno, M. Yamada, R. Mitamura, K. Ike, K. Toyama and M. Seki, *Analytical Chemistry*, 2013, 85, 7666−7673.
61. B. Nair Gourikutty Sajay, C.-P. Chang, H. Ahmad, P. Khuntontong, C. Chung Wong, Z. Wang, P. Daniel Puiu, R. Soo and A. R. Abdur Rahman, *Biomed Microdevices*, 2014, 16, 537–548.

62. A. Maton, J. Hopkins, C. W. McLaughlin, S. Johnson, M. Q. Warner, D. LaHart and J. D. Wright, *Human Biology and Health*, Prentice Hall, 1993.
63. E P Furlani, J. Phys. D: Appl. Phys. 40 (2007) 1313–1319
64. H.-K. Seo, H.-O. Kim and Y.-J. Kim, *Proceedings of 10th IEEE international conference on nanotechnology joint symposium with nano korea* 2010, 911-914.
65. K.-H. Han and A. B. Frazier, *NSTI-Nanotech 2005*, 2005.
66. K.-H. Han and A. B. Frazier, *JOURNAL OF MICROELECTROMECHANICAL SYSTEMS*, 2005, 14, 1057-7157.
67. K.-A. Hyun and H.-I. Jung, *Electrophoresis*, 2013, 34, 1028–1041.
68. L. Hajba and A. Guttman, *Trends in Analytical Chemistry*, 2014, 59, 9-16.
69. B. D. Plouffe, M. Mahalanabis, L. H. Lewis, C. M. Klapperich and S. K. Murthy, *Analytical Chemistry*, 2012, 84, 1336−1344.
70. K. Hoshino, Y.-Y. Huang, N. Lane, M. Huebschman, W. J. Uhr, P. E. Frenkel and Z. Xiaojing, *Lab Chip*, 2011, 11, 3449–3457.
71. K.-H. Han, A. Han and A. B. Frazier, *Biosensors and Bioelectronics*, 2006, 21, 1907–1914.
72. M. Safarikova and I. Safarik, *Letters in Applied Microbiology*, 2001, 33, 36-39.
73. T. Zhu , R. Cheng, S. A. Lee, E. Rajaraman, M. A. Eiteman, T. D. Querec, E. R. Unger and L. Mao, *Microfluid Nanofluid*, 2012, 13, 645–654.
74. O. Yassine, C. P. Gooneratne, D. Abu Smara, F. Li, H. Mohammed, J. Merzaban and J. Kosel, *Biomicrofluidics*, 2014, 8.
75. A. Ivon Rodrıguez-Villarreal, M. D. Tarn, L. A. Madden, J. B. Lutz, J. Greenman, J. Samitier and N. Pamme, *Lab on a Chip*, 2011, 11, 1240–1248.
76. D. Robert, N. Pamme, H. Conjeaud, F. Gazeau, A. Ilesb and C. Wilhelm, *Lab Chip*, 2011, 11, 1902.
77. J. Nam, H. Huang, H. Lim, C. Lim and S. Shin, *Analytical Chemistry*, 2013, 85, 7316−7323.
78. M. Glynn, D. Kirby, D. Chung, D. J. Kinahan, G. Kijanka and J. Ducrée, *Journal of Laboratory Automation*, 2013.
79. M. Karlel, J. Miwa, G. Roth, R. Zengerle and F. von Stetten, *Micro Electro Mechanical Systems, 2009. MEMS 2009. IEEE 22nd International Conference on*, 2009.
80. M. Karle, J. Miwa, G. Czilwik, V. Auwarter, G. Roth, R. Zengerle, F. von Stetten, Lab on a Chip, 2010, 10, 3284–3290.
81. M. Mizuno, M. Yamada, R. Mitamura, K. Ike, K. Toyama, M. Seki, Analytical Chemistry, 2013, 85, 7666−7673.
82. N. Han, J. Hwan Shin and K.-H. Han, *RSC Advances*, 2014, 4, 9160–9165.
83. S. Durdík, A. Krafcík, M. Babincová and P. Babinec, *Physica Medica*, 2013, 29, 562-567.
84. A. F. Sousa, J. Loureiro, M. M. Diogo, J. M. S. Cabral and P. P. Freitas, *Bioengineering (ENBENG), 2011. ENBENG 2011. 1st Portuguese Meeting in 1-4 March 2011*, 2011, 1 - 4.
85. J. Jung and K.-H. Han, *Transducers 2009, Denver, CO, USA, June 21-25, 2009*, 2009.

Biographies

Majid Hejazian is currently a PhD student with the Qeensland Micro- and Nanotechnology Centre at Griffith University, Australia. He received the BSc degree from the University of Isfahan and MSc degree in Chemical Engineering from Arak University in 2007 and 2013, respectively. His current research focus is the separation of cells and biological particles using magnetophoresis. His research interests include micro magnetofluidics, lab on a chip, computational fluid dynamics (CFD), fluid flow and heat transfer.

Weihua Li is a Professor with the School of Mechanical, Materials and Mechatronic Engineering of University of Wollongong, Australia. He received his B. E. and M. E. degrees from University of Science and Technology of China in 1992 and 1995 respectively, and Ph.D. degree from Nanyang Technological University (NTU) in 2001. He was a research fellow with NTU from 2001 to 2003. He has been with the University of Wollongong as a Lecturer (2003-2005), Senior Lecturer (2006-2009), Associate Professor (2010-2012), and Professor (2012-). Dr Li's research interests include but not limit to magnetorheological materials and their applications, microfluidics and nanofluidics.

Nam-Trung Nguyen a professor and the director of Queensland Micro and Nanotechnology Centre at Griffith University, Australia. He received his Dip-Ing, Dr Ing and Dr Ing Habil degrees from Chemnitz University of Technology, Germany, in 1993, 1997 and 2004, respectively. He was a postdoctoral research engineer with the Berkeley Sensor and Actuator Center, University of California at Berkeley, USA. From 1999 to 2013 he has been a Research Fellow, Assistant Professor and Associate Professor with Nanyang Technological University, Singapore. Dr. Nguyen has published over 220 journal papers and several books on microfluidics and nanofludics.

Lab on a Chip

Accepted Manuscript

ROYAL SOCIETY OF CHEMISTRY

www.rsc.org/loc